Title: Erythropoietin directly remodels the clonal composition of murine hematopoietic multipotent progenitor cells

A.S. Eisele[1], J. Cosgrove[1], A. Magniez[1], E. Tubeuf[1], S. Tenreira Bento[1], F. Cayrac[1], T. Tak[1], A.M. Lyne[1], J. Urbanus[3] and L. Perié[1*].

Affiliations

1. Institut Curie, Université PSL, Sorbonne Université, CNRS UMR168, Laboratoi re Physico Chimie Curie, 75005 Paris, France
2. Netherlands Cancer Institute, Amsterdam, Netherlands

Contact information

Leila Perié, Postal address: UMR168, Institute Curie, 11 rue Pierre et Marie Curie, 75005 Paris, Leila.Perie@curie.fr, +33156246229.

Abstract

The cytokine erythropoietin (EPO) is a potent inducer of erythrocyte development and one of the most prescribed biopharmaceuticals. The action of EPO on erythroid progenitor cells is well established, but its direct action on hematopoietic stem and progenitor cells (HSPCs) is still debated. Here, using cellular barcoding, we traced the differentiation of hundreds of single murine HSPCs, after *ex vivo* EPO-exposure and transplantation, in five different hematopoietic cell lineages, and observed the transient occurrence of high-output Myeloid-Erythroid-megaKaryocyte (MEK)-biased and Myeloid-B-cell-Dendritic cell (MBDC)-biased clones. Single-cell RNA sequencing (ScRNAseq) analysis of *ex vivo* EPO-exposed HSPCs corroborated our lineage tracing results, revealing that EPO induced the upregulation of erythroid associated genes in a subset of HSPCs, overlapping with multipotent progenitor (MPP) 1 and MPP2. Collectively, our data show that EPO does act directly on MPP independent of the niche, and modulates fate by remodeling the clonal composition of the MPP pool.

Introduction

Erythrocytes are the most numerous hematopoietic cells in our body and are constantly renewed[1]. The major inducer of erythroid cell development in steady state and anemic conditions is the cytokine EPO[2]. Recombinant EPO is widely used to treat anemia and is one of the most sold biopharmaceuticals[3]. Previously, EPO was thought to solely target erythroid-committed progenitors and induce their increased proliferation and survival via the EPO receptor (EPOR)[4]. Recently, EPO has also been suggested to act on HSPCs [5–12], but the nature of EPO´s effect on HSPC fate remains unresolved

despite potential adverse side effects during long-term EPO usage in the clinics and associations of high EPO levels with leukemias[13–15].

It is well established that EPO can induce HSPCs to cycle, as evidenced by a number of bulk and single cell studies *in vitro* and *in vivo*[5,12,8,9,11]. It's role in modulating HSPC fate is less clear however, with a lack of studies that functionally assess HSPC fate at the single cell level *in vivo*, and analyze the direct effect of EPO on HSPCs, and not the effect of the surrounding niche. More specifically, the upregulation of erythroid associated genes in HSPC (LSK CD150^{+} Flt3^{-} CD48^{-}) in response to *in vivo* EPO has been observed with bulk transcriptomics[11], suggesting that HSPCs deviate their fate toward erythroid production. Recent ScRNAseq analysis observed different changes of lineage-associated gene expressions after *in vivo* EPO-exposure of HSPCs[9,8]. As changes of gene expression do not necessarily result in cell fate modification[14], functional validations *in vivo* are necessary. In one study such functional validation was performed using bulk transplantation of *in vivo* EPO-exposed HSPCs (LSK CD150 Flt3^{-})[7]. This study showed increased erythroid production and decreased myeloid cell production, concluding that EPO deviates the fate of HSPCs in favor of erythroid production. As EPO has also been shown to target hematopoietic niche cells (osteoblasts and osteocytes[15,16] endothelial cells[17,16], adipocytes[18,19], and mesenchymal stem cells[6,20]), it remains however still unclear whether EPO acts directly on HSPCs, via their environment, or both.

It is now established that HSPCs encompass cells with different long-term reconstitution capacity after transplantation, as well as a heterogeneous output in terms of quantity (lineage-bias) and type of cells (lineage-restriction)[21–28]. Recently, the HSPC compartment was subdivided into long-term hematopoietic stem cells (LT-HSC) and different multipotent progenitors (MPP) (MPP1-4[29,30]), with variation around the

phenotypic definition[31]. Interestingly, HSPC composition responds to irradiation with HSC transiently self-renewing less and increasing their production of MPP2-3[31]. In the case of EPO, conflicting results suggest that either HSC or MPP respond to EPO [8,9,11] but the difference in HSPC definition and the lack of functional validation make it difficult to compare these studies. As HSPCs are functionally heterogeneous, and the current phenotypic definition partially capture this heterogeneity, a single cell in vivo lineage tracing approach is needed to assess whether EPO can influence HSPC fate decisions.

To analyze the functional effect of EPO on the differentiation of individual HSPCs (C-Kit$^+$ Sca1$^+$ CD150$^+$ Flt3$^-$) removing the effect of the niche, we here utilized cellular barcoding technology which allowed us to trace the progeny of hundreds of single HSPCs *in vivo*. By analyzing cellular barcodes in five mature hematopoietic lineages and HSPCs, we observed transient induction of high-output MEK-biased barcode clones compensated by MBDC-biased clones after ex vivo EPO-exposure. ScRNAseq of *ex vivo* EPO-exposed HSPCs revealed upregulation of erythroid associated genes in a subset of the compartment with overlap to gene signatures of MPP1 and MPP2 and not of LT-HSCs. Moreover, the increased contribution of biased HSPC clones to the mature cell lineages after EPO-exposure did not match their frequency in HSPCs, indicating that they were differentiating more than self-renewing, a property associated to multipotent progenitors. The transient effect of EPO on HSPCs further corroborates an action of EPO on MPP1/2 rather than LT-HSCs. Altogether our results are consistent with a model in which perturbations induce clonal remodeling of HSPC contributing to hematopoiesis, with biased MPPs transiently contributing more than LT-HSC. They also demonstrate a direct effect of EPO on MPPs after transplantation with implications for basic HSC research and therapeutic applications in the clinic.

Methods

Mice

Male C57BL/6J CD45.1^{+}, C57BL/6J CD45.2^{+}, and *Rosa26CreER*^{T2};*mT/mG* mice from Jackson Laboratory or bred at Institute Curie aged between 7-13 weeks were used in all experiments. All procedures were approved by the responsible national ethics committee (APAFIS#10955-201708171446318 v1).

Barcode library, barcode reference list and lentivirus production

The LG2.2 barcode library is composed of a DNA stretch of 180 bp with a 20 bp "N"-stretch. DsDNA was generated by 10 PCR rounds and cloned into the XhoI-EcoRI site of the lentiviral pRRL-CMV-GFP plasmid[32]. Subsequently ElectroMaxStbl4 cells were transformed, and >10,000 colonies picked for amplification by Maxiprep. To create the barcode reference list (https://github.com/PerieTeam/Eisele-et-al.-), barcode plasmids were PCR amplified twice in duplicate and sequenced as described below. Sequencing results were filtered as previously described in[33]. Lentiviruses were produced by transfecting the barcode plasmids and p8.9-QV and pVSVG into HEK293T cells in DMEM-Glutamax supplemented with 10% FCS (Gibco), 1% MEM NEAA, and 1% sodium pyruvate using Polyethyleneimine. Supernatant was 0,45 um filtered, concentrated by 1,5 h ultracentrifugation at 31,000g and frozen at -80°C.

HSPC isolation, barcoding, EPO treatment, and transplantation

Isolation and labeling of cells with the barcoding library was performed as described in[33]. Briefly, after isofluorane aneasthesia and cervical dislocation, bone marrow cells

were isolated from femur, tibia and iliac bones of mice by flushing, and C-Kit$^+$ cells were enriched with anti-CD117 magnetic beads on the MACS column system (Miltenyi). Cells were stained for C-kit, Flt3, CD150, Sca-1 (Table 1) and with Propidium iodide (PI) (Sigma) (1:5,000). HSPCs (Supplementary Figure 1a) were sorted and transduced with the barcode library in StemSpanMedium SFEM (STEMCELL Technologies) with 50 ng/ml mSCF (STEMCELL Technologies) through 1,5 h of centrifugation at 300 g and 4,5 h incubation at 37°C to obtain 10% barcoded cells. After transduction, cells were incubated with human recombinant EPO (Eprex, erythropoietin alpha, Janssen) at a final concentration of 1,000 or 160 ng/ml or PBS for 16 h at 37°C. After the incubation, the cells were transplanted by tail vein injection in recipient mice 6 Gy sub-lethally irradiated 3 hours before on a CIXD irradiator. Mice were randomly allocated to groups. When indicated, cells were injected together with additional EPO (16,000 IU/kg). On average 2,600 cells (Mean 2,684 cells +/- 175 cells) were injected in the tail vein of each mouse. A FACSAria™ (BD Biosciences) was used for sorting. FACSDiva™ software (BD Biosciences) was used for measurements and FlowJo™ v.10 (TreeStar) for analysis.

Cell progeny isolation for barcode analysis

Spleens were mashed and both blood and spleen cells were separated based on Ter119 using a biotinylated anti-Ter119 antibody (Table 1) and anti-biotinylated beads on the MACS column system (Miltenyi). Ter119$^+$ cells were stained for Ter119 and CD44[34]. Ter119$^-$ cells were stained for CD45.1 CD11b, CD11c, CD19, and if appropriate CD115, Siglec-F, and Ly6G (Table 1). Bone marrow cells were flushed from bones and enriched for C-Kit$^+$ cells as above. When appropriate the C-Kit$^-$ fraction was further separated based on Ter119 and stained as above. C-Kit$^+$ cells were stained

for C-Kit, Flt3, CD150, Sca-1, and if appropriate CD41 (Table 1), and PI (1:5000). For analyzed and/or sorted populations see Supplementary Figure 1a-d.

Lysis, barcode amplification and sequencing

Sorted cells were lysed in 40 µl Viagen Direct PCR Lysis Reagent (cell) (Euromedex) supplemented with 0,5 mg/ml Proteinase K Solution RNA grade (Invitrogen) at 55°C for 120 min, 85°C for 30 min, 95°C for 5 min. Samples were then split into two replicates, and a three-step nested PCR was performed (Primers and PCR program in Supplementary Method). PCR3 products for each sample and replicate were pooled, purified with the Agencourt AMPure XP system (Beckman Coulter), diluted to 5 nM. and sequenced on a HiSeq system (Illumina) (SR-65bp) at Institute Curie facility with 10% of PhiX spike-in.

Barcode sequence analysis

Sequencing results were filtered, and barcodes were categorized in progenitor classes as in[33]. In brief, read counts of each barcode in the different cell lineages were normalized enabling categorization into classes of biased output toward the analyzed lineages using a threshold of 10% of barcode reads (Other thresholds in Supplementary Figure 3c). Statistics on barcoding results were performed using a permutation test as in[35]. Significance of flow cytometry results was assessed using Student's T test.

ScRNAseq and analysis

ScRNAseq was performed using the 10X Genomics platform. Data was analyzed using Cellranger, Seurat[36] and customized scripts (Supplementary Method).

Data sharing statement

All codes and data are available at https://github.com/PerieTeam/Eisele-et-al.-

Contact author is leila.perie@curie.fr.

Results

EPO-exposure induces biases in single HSPCs. Given the debate surrounding which HSPC subset is responding to EPO, we decided to take an unbiased approach and analyzed the direct effect of EPO on the differentiation of HSPCs defined as C-Kit$^+$ Sca1$^+$ Flt3$^-$ CD150$^+$ (LT-HSC, MPP1 and MPP2), without subdividing them at the single cell level, by cellular barcoding. To this purpose, we generated a high-diversity lentiviral barcode library (LG2.2, 18,026 barcodes in reference list), consisting of random 20 nucleotides sequences positioned adjacent to the green fluorescent protein (GFP) gene, enabling the tracking of many individual cells in parallel. Using this LG2.2 library, we labeled single HSPCs (Supplementary Figure 1a) with unique genetic barcodes as previously described[33], exposed them to EPO (1,000 ng/ml) or PBS for 16 hours *ex vivo* and transplanted around 2,600 cells (Mean 2,684 cells +/- 175 cells) of which around 10% barcoded cells into irradiated mice (Figure 1a). Note that *ex vivo* exposed HSPC kept their original phenotype albeit a slight downregulation of C-Kit (Supplementary Figure 1f), which is known for cultures containing stem cell factor[37]. At day 30 after transplantation, the earliest timepoint at which HSPCs produce simultaneously erythroid, myeloid and lymphoid cells[38], barcoded (GFP$^+$) erythroblasts (E; Ter119$^+$ CD44$^+$[34]), myeloid cells (M; Ter119$^-$ CD19$^-$ CD11c$^-$ CD11b$^+$), and B-cells (B; Ter119$^-$ CD19$^+$) (Supplementary Figure 1b-c, e) were sorted from the spleen and their barcode identity assessed through PCR and deep-sequencing. Note that bone and spleen had similar barcoding profiles (Supplementary Figure 2). No difference in

chimerism was observed between the EPO and control group in the spleen and blood, even when mTdTomato/mGFP donor mice were used to better assess the erythroid lineage (Figure 1b-c). On average, we detected around eighty barcodes per mouse, of which most were detected in several lineages (Figure 1d). Comparison of the numbers of barcodes producing each lineage showed that EPO-exposure resulted in the same number of engrafting and differentiating cells as in control (Figure 1d). Notably, the number of erythroid restricted cells remained stable in the EPO group as compared to control (Figure 1e), indicating that the response to EPO is more complex than a direct instruction of erythroid-restricted HSPCs.

To quantify the effect of EPO on HSPC lineage-biases, barcode-labeled HSPCs were classified based on the balance of their cellular output in the M, B and E lineages. With this classification using a 10% threshold, cells classify for example as ME-biased if they have above 10% of their output in the M and E lineage, and under 10% of their output in the B lineage (Supplementary Figure 3b, other thresholds in Supplementary Figure 3c). Interestingly, application of this classification revealed that although the proportion of lineage-biased HSPCs in control and EPO group was similar (Figure 1f), their contribution to the different lineages was increased by EPO-exposure (Figure 1g). In the control group, balanced HSPCs (MBE) produced the majority of all lineages, as previously published[39]. In the EPO group, ME- and MB-biased clones produced most cells of the analyzed lineages (Figure 1g). ME-biased HSPCs produced the majority of erythroid cells (57% +/- 10%), MB-biased HSPCs produced the majority of B-cells (58% +/- 36%), and ME- and MB-biased clones contributed the majority of myeloid cells (MB-biased 45% +/- 38% and ME-biased 20% +/- 13%, together 65% +/- 25%). To test the significance of this effect, we used a permutation test, which compares the effect size between control and EPO group to the one of all random groupings of

mice[35]. The contributions of the ME- and of the MB-biased HSPC classes to the different lineages were significantly different in EPO and control groups (Supplementary Table 1). These results were reproduced in an additional experiment (Supplementary Figure 3c-g). A lower EPO concentration (160 ng/ml) as well as an additional single injection of EPO (16,000 IU/kg) during transplantation gave similar results (Figure 2, Supplementary Figure 4, Supplementary Table 1). Also at six weeks post transplantation, similar results were obtained (Supplementary Figure 5). In summary, *ex vivo* EPO priming of HSPCs modified the output balance of HSPCs rather than the clonal composition of lineage-restricted and -biased cells. Balanced clones produced a smaller percentage of the mature cells; ME-biased HSPCs produced most of the erythroid cells and MB-biased HSPCs produced most of the B cells.

Contribution of ME- and MB-biased HSPCs to the DC and MkP lineage. To further characterize the cells produced by the ME-biased and MB-biased HSPCs, we repeated our experimental setup including the analysis of the megakaryocyte and dendritic cell (DC) lineages (Figure 3). Megakaryocyte Progenitors (MkP) were chosen as proxy for the production of platelets which are not suitable for barcode analysis. Barcoded (GFP^+) DCs (DC; Donor $Ter119^-$ $CD19^-$ $CD11c^+$ $CD11b^-$) and MkP (MkP; C-Kit^+ Sca-1^- $CD150^+$ $CD41^+$) (Supplementary Figure1 c-e) were sorted together with M, E, and B cells, 4 weeks after transplantation of control or EPO-exposed HSPCs (1,000 ng/ml). In both groups, the majority of clones produced also DCs (Figure 3a). In the control group, balanced HSPCs produced the majority of DCs (65% +/- 9%) (Figure 3b). However, in the EPO group, balanced HSPCs decreased their contribution to the DC lineage (36% +/-25%) and MB-biased HSPCs significantly increased their contribution (86% +/- 43% EPO vs 22% +/- 11% control group) (Figure 3b, Supplementary Table

1), thus, they were MBDC-biased HSPCs. In contrast the ME-biased HSPCs produced few DCs in both groups (Figure 3b), indicating that ME-biased HSPCs are restricted both in their B and DC production compared to the M and E production.

The majority of the MkP production came from the ME-biased HSPCs in both groups (58% +/- 21% control and 55% +/- 14% EPO group, Figure 3c-d), indicating that ME-biased HSPCs were also MkP-biased HSPCs (thus MEK-biased). We did not detect a high contribution of MkP-restricted HSPCs[25,24,40] to the MkP lineage (Figure 3d). Finally, as high EPO-exposure has been linked to changes in macrophage numbers[41–48] we analyzed the contribution of control and EPO-exposed HSPCs to the myeloid lineage in more detail, but could not detect changes in the percentage of the different myeloid subsets produced (Supplementary Figure 6a-c).

Effect of EPO on HSPC self-renewal. In light of previous studies which suggested changes in HSPC proliferation after *in vivo* EPO-exposure[5,12,8,9,11], we next explored if the self-renewal capacity of HSPCs was impacted. To this end, we analyzed barcodes in bone marrow HSPCs in addition to the spleen E, M, and B lineages at week 4 after transplantation of control or EPO-exposed HSPCs (160 and 1,000 ng/ml) (Figure 4).

We reasoned that barcodes of HSPCs self-renewing and differentiating after transplantation are detected in both compartments, while detection in only HSPCs or mature lineages indicates a prevalence of self-renewal or differentiation respectively. Most of the barcodes detected in HSPCs overlapped with barcodes in the mature cells (Figure 4b left) in both the control and two EPO groups, showing that most of the transplanted cells were self-renewing and differentiating irrespective of the treatment. Some barcodes were only detected in mature cells (Figure 4b right), indicating that

some HSPCs had not self-renewed or were below the limit of detection. These HSPCs were equally abundant in the control and two EPO groups (Figure 4b right).

To analyze if different lineage biases correlated to different self-renewal capacity, we analyzed the proportion of biased HSPC classes, as previously defined, within the HSPC compartment (Figure 4c). In the control group, balanced and ME-biased HSPCs contributed most to the HSPC reads (34% +/- 36% MBE and 37% +/- 34% ME-biased HSPCs), while barcodes of MB-biased HSPCs contributed less (15% +/- 32%) (Figure 4c), a trend that has been previously described[49,50,25]. Surprisingly, the pattern of contributions of different biased HSPC subsets to HSPC reads was unchanged in the EPO groups (Figure 4c), implying that the extent of self-renewal was unchanged after *ex vivo* EPO-exposure.

To study if the increased production of cells by the ME- and MB-biased HSPCs to the mature cells observed after *ex vivo* EPO-exposure (Figure 1-3) correlated with self-renewal capacity of HSPCs, we analyzed the contribution of barcodes detected or not in HSPCs to the E, M, and B lineages (Figure 4d). In the control group, the majority of mature cells were derived from barcodes also present in HSPCs. However, in both EPO groups, the contribution of barcodes detected in HSPCs to mature cells was significantly lower (Figure 4d, Supplementary Table 1) implying that the increased contribution of biased HSPC classes to the mature cell lineages after *ex vivo* EPO-exposure was most likely caused by cells differentiating more than self-renewing.

EPO-exposure induces an erythroid program in a subgroup of HSPCs. To further characterize the effect of EPO-exposure on HSPCs, we performed scRNAseq of barcoded C-Kit^{+} Sca1^{+} Flt3^{-} CD150^{+} cells after *ex vivo* culture in medium supplemented with EPO or PBS using the 10X Genomics platform. 1,706 cells from control and 1,595

cells from the EPO group passed our quality control. To compare the HSPCs injected with non-cultured hematopoietic cells, we generated a reference map of 44,802 C-kit^{+} cells from[51] and used published signatures as detailed in the supplementary materials and methods[31,52] to annotate this map (Supplementary Figure 7a,b and e,f). Projection of our single cell data on this map showed that both the control and the EPO-exposed HSPCs similarly overlapped with non-MPP4 LSK cells, according to their sorting phenotype (Supplementary Figure 7e,f). These results indicate that neither the *ex vivo* culture itself nor the EPO treatment dramatically affected the global identity of the sorted HSPCs.

When comparing the EPO and control group, we found 1,176 differentially expressed genes (Figure 5a and Supplementary Table 2) and this number was significantly higher than the number expected due to chance (p-value=0,01) as assessed by permutation testing. Among the most upregulated genes in the EPO-exposed HSPCs, were genes with erythroid association as *Hbb-bs*, *Erdr1*, *Wtap*, *Kmt2d*, or *Nfia*[53], and GATA1 targets (*Abhd2*, *Cbx3*, *Kdelr2*, *Pfas*), cell cycle related genes (*Tubb5*, *Hist1h2ap*) as well as genes previously described to be induced in HSPCs after *in vivo* EPO-exposure, such as *Bmp2k*[6] and *Ifitm1*[8] (Figure 5c). Genes involved in stem cell maintenance, such as *Serpina3g*, *Mecom, Txnip*, *Meis1*, *Pdzk1ip1*[8], *Sqstm1*[54], *Smad7*[55], *Aes*[56], were among the most downregulated genes in the EPO-exposed HSPCs (Figure 5a).

As our cellular barcoding data suggests that single HSPCs differ in their response to EPO, we assessed the heterogeneity of EPO responses at the transcriptomic level. UMAP-based visualization of the data suggested that a subgroup of EPO-exposed cells was transcriptomically distinct (Figure 5b), independently of the number of PCA components and genes used in the analysis (Supplementary Figure 7c). To test this

observation, we defined an EPO response signature based on differentially expressed genes between the EPO and control group. Plotting the expression of the EPO response signature at the single cell level showed that the majority of the transcriptomic differences between the control and EPO group were indeed driven by this small subgroup of cells (Figure 5c). Reasoning that this subgroup contains the cells directly responding to EPO, we defined as EPO-responders, cells in the 90th percentile of EPO response signature expression (Figure 5c) for subsequent analysis. Importantly, unsupervised clustering analysis of the data (Supplementary Figure 8a-b) showed similar results. The genes encoding EPOR, as well as the alternative EPO receptors EphB4, CD131, CRFL3 were equally expressed between the EPO-responders, non-responders and control groups (Supplementary Figure 7d). Reasoning that the EPO-responders correspond to MEK-biased HSPCs, we also looked for potential MBDC-biased HSPCs but could not detect a subgroup of cells with upregulation of lymphoid associated genes, suggesting that the MBDC-bias is not a direct effect of EPO-exposure but more an indirect effect. In summary, the scRNAseq analysis corroborated our functional barcoding data, showing that a subset of HSPCs can respond directly to EPO stimulation.

EPO-responder HSPCs overlap with MPP1 and MPP2 signatures. As our barcode analysis suggested that the effect of direct EPO-exposure on HSPCs is caused by cells differentiating more than self-renewing, we next wanted to assess which of the HSPC subsets are the EPO responders in our scRNAseq dataset. We annotated the UMAP-based visualization of our data with published signatures of the HSC (dormant HSCs[57] and LT-HSC[58]), MPP1[57] and MPP2[31] subsets included in our HSPC gate, and analyzed its overlap with the previously defined EPO-responder and non-responder

cells (Figure 6a,b). Relative to the control group and non-responders of the EPO-group, the EPO-responders had a reduced expression of HSC gene signatures and increased expression of MPP1 and MPP2 signatures (Figure 6a,b). An annotation of the reference map generated from data of[51] likewise showed a low overlap of EPO-responders with the most quiescent HSC subsets (Figure 6c,d). The independent analysis using unsupervised clustering further supported this result (Supplementary Figure 8c,d). All in all, our scRNAseq analysis implied that, in line with our barcoding results, the HSPCs directly reacting to EPO are most likely multipotent progenitor cells of the MPP1 and MPP2 subsets.

Transient effect of EPO-exposure.

Finally, we reasoned that if EPO directly acts on multipotent progenitors MPP1/2 with short reconstitution capacity after transplantation rather than long-term repopulating HSC, then the EPO effect should be transient. To test this hypothesis, we repeated the experiment and analyzed barcodes in the E, M, and B lineages at 4 months after transplantation of control or EPO-exposed HSPCs (160 and 1,000 ng/ml) (Fig. 7). In the control group, as reported before[59], the chimerism at 4 months was higher and the number of barcodes detected was lower than at one month post-transplantation (Fig. 7c-d and 1b-d). We detected no significant changes in the clonal output of HSPCs between control and EPO group at this timepoint (Fig. 7e), with the majority of cells in all lineages produced by balanced HSPCs (Fig. 7a-b), implying that the effect of direct EPO-exposure on HSPCs is transient. This confirms that the effect of direct EPO-exposure on HSPCs is likely caused by multipotent progenitor cells with a short reconstitution capacity after transplantation.

Discussion

By analyzing the functional effect of EPO on the differentiation of individual HSPCs, removing the effect of the niche, we could establish that EPO has a direct effect on the differentiation of individual C-Kit$^+$ Sca1$^+$ Flt3$^-$ CD150$^+$ HSPCs. EPO induced MEK-biased and MBDC-biased HSPCs that produced the majority (>60%) of mature hematopoietic cells at four and six weeks after transplantation. The increased erythroid-associated gene signature in a subset of HSPCs after *ex vivo* EPO-exposure suggests that EPO directly induces high output MEK-biased HSPCs, which is indirectly compensated for by occurrence of MBDC-biased HSPCs to maintain a balanced production of hematopoietic cells. These biased clones have properties of multipotent progenitors and not LT-HSC as shown by their propension to differentiate more than self-renewing, their expression of MPP1 and MPP2 gene signature and their transient response post-transplantation.

Similar to studies that have used high systemic EPO-exposure on HSPC[10,9,11,8], we found that multipotent progenitors are responding to EPO instead of HSC, implying that this property is not governed by the niche. However, we did not detect a fate deviation toward erythroid production at the expense of myeloid production as seen for in vivo EPO-exposed HSPCs after transplantation[7]. We observed a more complex remodeling of the clone contributing to hematopoiesis in response to EPO, with a transiently increased contribution of biased MPPs. This is in line with a model in which MPP serve as a transient compartment for rapid expansion in response to stimulation[31]. The direct effect of EPO on MPPs we described here could be one of the factors underlying the development of adverse side effects and co-morbidities during long-term EPO use in the clinics and associations of high EPO levels with leukemias[60,13,61].

Acknowledgements

We thank Dr. T. Schumacher for discussion and lentiviral library production and Dr. K Duffy for advices on permutation testing. We thank the Institute Curie flow cytometry, next generation sequencing, and animal facility. We thank Fahima Di Federico from the UMR168 BMBC facility for amplifying the barcode plasmid pool. A.S.E was supported by the IC-3i International PhD program of Institut Curie, in part funded by the European Commission´s MSCA COFUND scheme under the Marie Sklodowska-Curie Grant Agreement No 666003, and the Frontières de l´Innovation en Recherche et Education (FIRE) doctoral school of the Centre for Interdisciplinary research (CRI) Paris (Ecole doctroale n° 474, former Frontières du Vivants). The study was supported by an ATIP-Avenir grant from CNRS and Bettencourt-Schueller Foundation (to L.P.) and two grants from the *Labex CelTisPhyBio* (ANR-11-LABX-0038) and Idex Paris-Science-Lettres Program (ANR-10-IDEX-0001-02 PSL) (to L.P.). It was also supported by a starting ERC grant from the H2020 program (758170-Microbar to L.P.).

Authorship Contributions

A.S.E designed experiments, performed experiments, and analyzed data; A.M, E.T and S.T.B performed experiments; T.T performed experiments and advised experiment design; J.C performed scRNAseq analysis with the feedback from A.M.L; J.U designed and made the lentiviral library under supervision; F.C produced the lentiviral library DNA stock; L.P designed experiment, advised data analysis and supervised the study; A.S.E and L.P wrote the paper, incorporating feedback from all coauthors.

Disclosure of Conflict of interest

The authors declare no competing interests.

References

1. Sender R, Fuchs S, Milo R. Are We Really Vastly Outnumbered? Revisiting the Ratio of Bacterial to Host Cells in Humans. *Cell*. 2016;164(3):337–40.
2. Richmond TD, Chohan M, Barber DL. Turning cells red: signal transduction mediated by erythropoietin. *Trends Cell Biol.* 2005;15(3):146–155.
3. Walsh G. Biopharmaceutical benchmarks 2014. *Nat. Biotechnol.* 2014;32(10):992–1000.
4. Koury MJ. Tracking erythroid progenitor cells in times of need and times of plenty. *Exp. Hematol.* 2016;44(8):653–63.
5. Cheshier SH, Prohaska SS, Weissman IL. The effect of bleeding on hematopoietic stem cell cycling and self-renewal. *Stem Cells Dev.* 2007;16(5):707–17.
6. Shiozawa Y, Jung Y, Ziegler AM, et al. Erythropoietin Couples Hematopoiesis with Bone Formation. *PLoS One*. 2010;5(5):e10853.
7. Grover A, Mancini E, Moore S, et al. Erythropoietin guides multipotent hematopoietic progenitor cells toward an erythroid fate. *J. Exp. Med.* 2014;211(2):181–188.
8. Giladi A, Paul F, Herzog Y, et al. Single-cell characterization of haematopoietic progenitors and their trajectories in homeostasis and perturbed haematopoiesis. *Nat. Cell Biol.* 2018;1.
9. Yang J, Tanaka Y, Seay M, et al. Single cell transcriptomics reveals unanticipated features of early hematopoietic precursors. *Nucleic Acids Res.* 2017;45(3):1281–1296.
10. Tusi BK, Wolock SL, Weinreb C, et al. Population snapshots predict early haematopoietic and erythroid hierarchies. *Nature*. 2018;555(7694):54–60.
11. Singh RP, Grinenko T, Ramasz B, et al. Hematopoietic Stem Cells but Not Multipotent Progenitors Drive Erythropoiesis during Chronic Erythroid Stress in EPO Transgenic Mice. *Stem Cell Reports*. 2018;10(6):1908–1919.
12. Dubart A, Feger F, Lacout C, et al. Murine pluripotent hematopoietic progenitors constitutively expressing a normal erythropoietin receptor proliferate in response to erythropoietin without preferential erythroid cell differentiation. *Mol. Cell. Biol.* 1994;14(7):4834–42.
13. Ma W, Kantarjian H, Zhang K, et al. Significant association between polymorphism of the erythropoietin gene promoter and myelodysplastic syndrome. *BMC Med. Genet.* 2010;11(1):163.
14. Weinreb C, Rodriguez-Fraticelli A, Camargo FD, Klein AM. Lineage tracing on transcriptional landscapes links state to fate during differentiation. *Science*. 2020;
15. Li C, Shi C, Kim J, et al. Erythropoietin Promotes Bone Formation through EphrinB2/EphB4 Signaling. *J. Dent. Res.* 2015;94(3):455–463.
16. Singbrant S, Russell MR, Jovic T, et al. Erythropoietin couples erythropoiesis, B-lymphopoiesis, and bone homeostasis within the bone marrow microenvironment. *Blood*. 2011;117(21):.
17. Ito T, Hamazaki Y, Takaori-Kondo A, Minato N. Bone Marrow Endothelial Cells

Induce Immature and Mature B Cell Egress in Response to Erythropoietin. *Cell Struct. Funct.* 2017;42(2):149–157.
18. American Society of Hematology S, Alvarez JC, Noguchi CT. Blood. American Society of Hematology; 2017.
19. Zhang Y, Wang L, Dey S, et al. Erythropoietin action in stress response, tissue maintenance and metabolism. *Int. J. Mol. Sci.* 2014;15(6):10296–333.
20. Tari K, Atashi A, Kaviani S, et al. Erythropoietin induces production of hepatocyte growth factor from bone marrow mesenchymal stem cells in vitro. *Biologicals*. 2017;45:15–19.
21. Dykstra B, Kent D, Bowie M, et al. Long-Term Propagation of Distinct Hematopoietic Differentiation Programs In Vivo. *Cell Stem Cell*. 2007;1(2):218–229.
22. Morita Y, Ema H, Nakauchi H. Heterogeneity and hierarchy within the most primitive hematopoietic stem cell compartment. *J. Exp. Med.* 2010;
23. Oguro H, Ding L, Morrison SJ. SLAM family markers resolve functionally distinct subpopulations of hematopoietic stem cells and multipotent progenitors. *Cell Stem Cell*. 2013;13(1):102–16.
24. Sanjuan-Pla A, Macaulay IC, Jensen CT, et al. Platelet-biased stem cells reside at the apex of the haematopoietic stem-cell hierarchy. *Nature*. 2013;502(7470):232–6.
25. Carrelha J, Meng Y, Kettyle LM, et al. Hierarchically related lineage-restricted fates of multipotent haematopoietic stem cells. *Nature*. 2018;554(7690):106–111.
26. Yamamoto R, Morita Y, Ooehara J, et al. Clonal analysis unveils self-renewing lineage-restricted progenitors generated directly from hematopoietic stem cells. *Cell*. 2013;154(5):1112–1126.
27. Lu R, Neff NF, Quake SR, Weissman IL. Tracking single hematopoietic stem cells in vivo using high-throughput sequencing in conjunction with viral genetic barcoding. *Nat. Biotechnol.* 2011;29(10):928–33.
28. Verovskaya E, Broekhuis MJC, Zwart E, et al. Heterogeneity of young and aged murine hematopoietic stem cells revealed by quantitative clonal analysis using cellular barcoding. *Blood*. 2013;122(4):523–532.
29. Wilson A, Laurenti E, Oser G, et al. Hematopoietic Stem Cells Reversibly Switch from Dormancy to Self-Renewal during Homeostasis and Repair. *Cell*. 2008;135(6):1118–1129.
30. Cabezas-Wallscheid N, Klimmeck D, Hansson J, et al. Identification of regulatory networks in HSCs and their immediate progeny via integrated proteome, transcriptome, and DNA methylome analysis. *Cell Stem Cell*. 2014;15(4):507–522.
31. Pietras EM, Reynaud D, Kang Y-A, et al. Functionally Distinct Subsets of Lineage-Biased Multipotent Progenitors Control Blood Production in Normal and Regenerative Conditions. *Cell Stem Cell*. 2015;17(1):35–46.
32. Dull T, Zufferey R, Kelly M, et al. A Third-Generation Lentivirus Vector with a Conditional Packaging System. *J. Virol.* 1998;72(11):8463.
33. Naik SH, Perié L, Swart E, et al. Diverse and heritable lineage imprinting of early haematopoietic progenitors. *Nature*. 2013;496(7444):229–232.
34. Chen K, Liu J, Heck S, et al. Resolving the distinct stages in erythroid differentiation based on dynamic changes in membrane protein expression during erythropoiesis. *Proc. Natl. Acad. Sci.* 2009;106(41):17413–17418.
35. Tak T, Prevedello G, Simon G, et al. Simultaneous tracking of division and

differentiation from individual hematopoietic stem and progenitor cells reveals within-family homogeneity despite population heterogeneity. *bioRxiv*. 2019;586354.
36. Satija R, Farrell JA, Gennert D, Schier AF, Regev A. Spatial reconstruction of single-cell gene expression data. *Nat. Biotechnol.* 2015;33(5):495–502.
37. Matsuoka Y, Sasaki Y, Nakatsuka R, et al. Low level of C-kit expression marks deeply quiescent murine hematopoietic stem cells. *Stem Cells*. 2011;29(11):1783–1791.
38. Boyer SW, Rajendiran S, Beaudin AE, et al. Clonal and Quantitative In Vivo Assessment of Hematopoietic Stem Cell Differentiation Reveals Strong Erythroid Potential of Multipotent Cells. *Stem Cell Reports*. 2019;12(4):801–815.
39. Perié L, Duffy KR, Kok L, de Boer RJ, Schumacher TN. The Branching Point in Erythro-Myeloid Differentiation. *Cell*. 2015;163(7):1655–62.
40. Rodriguez-Fraticelli AE, Wolock SL, Weinreb CS, et al. Clonal analysis of lineage fate in native haematopoiesis. *Nat. Publ. Gr.* 2018;553:.
41. Theurl I, Hilgendorf I, Nairz M, et al. On-demand erythrocyte disposal and iron recycling requires transient macrophages in the liver. *Nat. Med.* 2016;22(8):945–51.
42. Wang J, Hayashi Y, Yokota A, et al. Expansion of EPOR-negative macrophages besides erythroblasts by elevated EPOR signaling in erythrocytosis mouse models. *Haematologica*. 2018;103(1):40–50.
43. Gilboa D, Haim-Ohana Y, Deshet-Unger N, et al. Erythropoietin enhances Kupffer cell number and activity in the challenged liver. *Sci. Rep.* 2017;7(1):10379.
44. Kuzmac S, Grcevic D, Sucur A, Ivcevic S, Katavic V. Acute hematopoietic stress in mice is followed by enhanced osteoclast maturation in the bone marrow microenvironment. *Exp. Hematol.* 2014;42(11):966–975.
45. Ulyanova T, Phelps SR, Papayannopoulou T. The macrophage contribution to stress erythropoiesis: when less is enough. *Blood*. 2016;128(13):1756–65.
46. Mausberg AK, Meyer Zu Hörste G, Dehmel T, et al. Erythropoietin ameliorates rat experimental autoimmune neuritis by inducing transforming growth factor-β in macrophages. *PLoS One*. 2011;6(10):e26280.
47. Liao C, Prabhu KS, Paulson RF. Monocyte derived macrophages expand the murine stress erythropoietic niche during the recovery from anemia. *Blood*. 2018;blood-2018-06-856831.
48. Bretz CA, Divoky V, Prchal J, et al. Erythropoietin Signaling Increases Choroidal Macrophages and Cytokine Expression, and Exacerbates Choroidal Neovascularization. *Sci. Rep.* 2018;8(1):2161.
49. Kim S, Kim N, Presson AP, et al. Dynamics of HSPC repopulation in nonhuman primates revealed by a decade-long clonal-tracking study. *Cell Stem Cell*. 2014;
50. Aiuti A, Biasco L, Scaramuzza S, et al. Lentiviral hematopoietic stem cell gene therapy in patients with wiskott-aldrich syndrome. *Science (80-.).* 2013;341(6148):.
51. Dahlin JS, Hamey FK, Pijuan-Sala B, et al. A single-cell hematopoietic landscape resolves 8 lineage trajectories and defects in Kit mutant mice. *Blood*. 2018;131(21):e1–e11.
52. Wolf FA, Hamey FK, Plass M, et al. PAGA: graph abstraction reconciles clustering with trajectory inference through a topology preserving map of single

cells. *Genome Biol.* 2019;
53. Starnes LM, Sorrentino A, Pelosi E, et al. NFI-A directs the fate of hematopoietic progenitors to the erythroid or granulocytic lineage and controls β-globin and G-CSF receptor expression. *Blood*. 2009;114(9):1753–1763.
54. Meenhuis A, Van Veelen PA, De Looper H, et al. MiR-17/20/93/106 promote hematopoietic cell expansion by targeting sequestosome 1-regulated pathways in mice. *Blood*. 2011;118(4):916–925.
55. Blank U, Karlsson G, Moody JL, et al. Smad7 promotes self-renewal of hematopoietic stem cells. *Blood*. 2006;
56. Steffen B, Knop M, Bergholz U, et al. AML1/ETO induces self-renewal in hematopoietic progenitor cells via the Groucho-related amino-terminal AES protein. *Blood*. 2011;117(16):4328–4337.
57. Cabezas-Wallscheid N, Buettner F, Sommerkamp P, et al. Vitamin A-Retinoic Acid Signaling Regulates Hematopoietic Stem Cell Dormancy. *Cell*. 2017;
58. Wilson NK, Kent DG, Buettner F, et al. Combined Single-Cell Functional and Gene Expression Analysis Resolves Heterogeneity within Stem Cell Populations. *Cell Stem Cell*. 2015;
59. Wu C, Espinoza DA, Koelle SJ, et al. Geographic clonal tracking in macaques provides insights into HSPC migration and differentiation. *J. Exp. Med.* 2018;215(1):217–232.
60. Rainville N, Jachimowicz E, Wojchowski DM. Targeting EPO and EPO receptor pathways in anemia and dysregulated erythropoiesis. *Expert Opin. Ther. Targets*. 2016;20(3):287–301.
61. Halawi R, Cappellini MD, Taher A. A higher prevalence of hematologic malignancies in patients with thalassemia: Background and culprits. *Am. J. Hematol.* 2017;92(5):414–416.

Tables

Table 1: Fluorescently labeled antibodies

Antibody target	Clone	Conjugate	Manufacturer
CD45.1	A20	PE	BD Biosciences
Ter119	TER119	PE-Cy7	BD Biosciences
CD11c	N418	APC	eBioscience
CD19	1D3	APC-Cy7	BD Biosciences
CD11b	M1/70	PerCP-Cy5.5	eBioscience
CD117 (C-Kit)	2B8	APC	BioLegend
CD135 (Flt3)	A2F10	PE	eBioscience
CD135 (Flt3)	A2F10	PE-Cy5	Life technologies

Sca1	D7	Pacific Blue	BioLegend
CD150	TC15-12F12.2	PE-Cy7	BioLegend
Ter119	TER119	biotin	BD Biosciences
CD44	IM7	PE	BD Biosciences
CD41	MVVREG30	BV510	BD Biosciences
Siglec-F	E50-2440	PE-CF594	BD biosciences
Ly6G	1A8	BV510	BioLegend
CD115	AFS98	PE	BioLegend

Figure Legends

Figure 1: High output ME- and MB-biased clones occur after EPO-exposure and transplantation of HSPCs. **a**, HSPCs were sorted from the bone marrow of donor mice, lentivirally barcoded, cultured *ex vivo* with or without 1,000 ng/ml EPO for 16 h and transplanted into sublethally irradiated mice. At week 4 post-transplantation, the erythroid (E), myeloid (M), and B-cells (B) lineages were sorted from the spleen and processed for barcode analysis. **b**, The percentage of donor derived cells (CD45.1$^+$) among the total spleen, myeloid cells (CD11b$^+$) or B-cells (CD19$^+$) in the spleen of control and EPO group. **c**, To better assess chimerism in erythroid cells mTdTomato/mGFP donor mice were used. The fraction of Tom$^+$ cells among erythroid cells (Ter119$^+$) in the spleen and blood in control and EPO group. **d**, Number of barcodes retrieved in the indicated lineages at week 4 after transplantation in control and EPO group. **e**, Triangle plots showing the relative abundance of barcodes (circles) in the E, M, and B lineage with respect to the summed output over the three lineages (size of the circles) for control and EPO group. **f**, Percentage of HSPCs classified by the indicated lineage bias, using a 10% threshold for categorization. **g**, Quantitative contribution of the classes as in f to each lineage. Shown are values from several animals (n= 8 EPO, n= 10 control in b, n= 3 EPO, n=4 control in c spleen, n= 4 EPO, n=8 control in c blood collected over 5 different experiments (d-g) n=5 for control and n=2 for EPO group collected over one experiment). For all bar graphs mean and S.D. between mice are depicted. Statistical significance tested using Student-T-test p=0,05

for (b-c). Statistical significance tested by permutation test for g (see Supplementary Table 1).

Figure 2: Effect of different EPO concentrations on HSPC clonality after transplantation. Same protocol as in Figure 1 but HSPCs were cultured with different concentrations of EPO (160 ng/ml or 1,000 ng/ml) for 16 h, and when indicated a single dose of EPO (16,000 IU/kg) was injected together with barcoded cells at the moment of transplantation. **a**, Triangle plots showing the relative abundance of barcodes (circles) in the erythroid (E), myeloid (M), and B-lymphoid (B) lineage with respect to the summed output over the three lineages (size of the circles) for the different experimental groups as indicated. **b**, The percentage of each lineage produced by the barcodes categorized by bias using a 10% threshold. Shown are values from several animals (n=2 for 160 ng/ml, 1,000 ng/ml, and 160 ng/ml + EPO injection, n=4 for 1,000 ng/ml + EPO injection (collected over 4 different experiments)). For all bar graphs mean and S.D. between mice are depicted. Statistical significance tested by permutation test for different subsets in b (see Supplementary Table 1).

Figure 3: Production of Dendritic Cells (DC) and Megakaryocyte Progenitors (MkP) by HSPCs after EPO-exposure and transplantation. In addition to the analysis of barcodes in the erythroid (E), the myeloid (M), and the B-cell (B) lineage, the DC lineage in spleen and MkP in bone marrow were added. **a**, Percentage of barcoded HSPCs producing DC in the different HSPC categories (classification as in Figure 2 based on the M, E, and B lineage only using a 10% threshold. The DC only category was added). **b**, The percentage of the DC lineage produced by the barcodes categorized by bias as in a. **c-d**, Representations as in a-b for barcode detection in MkP. Data is derived from a cohort with detailed myeloid sorting. The myeloid lineage was merged according to the percentage of total donor myeloid each subset contributed as in Supplementary Figure 4a to allow classification as in a-b based on the M, E, and B lineage only using a 10% threshold. The MkP only category was added. Shown are values from several animals (a-b, n=5 for control and n=2 for EPO group, c-d, n=3 for control and n=1 for EPO group (collected over two experiments)). For all bar graphs mean and S.D. between mice are depicted. Statistical significance tested using Student-T-test p=0,05 for (a,c). Statistical significance tested by permutation test for different subsets in b (see Supplementary Table 1).

Figure 4: Overlap of barcodes in HSPCs and mature cells after transplantation of EPO-exposed HSPCs. Same protocol as in Figure 1 but HSPCs were cultured with two different concentrations of EPO (160 ng/ml or 1000 ng/ml) for 16 h. In addition, HSPCs were sorted and subjected to barcode analysis. **a**, The total number of barcodes found back in HSPCs. **b**, The percentage of barcodes in the mature cell subsets also detected in HSPCs and the percentage of barcodes in HSPCs also detected in mature cells. **c**, The percentage of the HSPC lineage contributed by barcodes categorized by bias as in Figure 2 based on the M, E, and B lineage using a 10% threshold. **d**, The percentage of each lineage produced by the barcodes color coded for presence (blue) and absence (grey) in HSPCs. Shown are values from several animals (n=5 for control, n=2 for EPO 160 ng/ml group and n=3 for EPO 1,000 ng/ml group). For all bar graphs mean and S.D. between mice are depicted. Statistical significance tested using Student-T-test p=0,05 for (a-b). Statistical significance tested by permutation test for different subsets in d (see Supplementary Table 1).

Figure 5: Characterization of EPO-exposed HSPCs by scRNAseq. HSPCs were sorted, barcoded and cultured *ex vivo* with or without 1,000 ng/ml EPO for 16 h, and analysed by scRNAseq using the 10X Genomics platform. 1,706 cells from control and 1,595 cells from EPO group passed quality control **a**, Volcano plot of log2 fold change of the differentially expressed genes between control and EPO-exposed cells versus the adjusted p-value. Genes of interest are annotated. Differentially expressed genes were used to defined an EPO response signature. **b**, UMAP visualization of the EPO-exposed and control HSPCs. **c**, The level of expression in the EPO-exposed HSPCs of the genes in the EPO response signature (top), and definition of the EPO-responder and non-responder subgroups using the 90th percentile expression of the EPO response signature from c (bottom). **d**, The expression of the indicated genes in the control, EPO-responder and non-responder subgroups as defined in c. Genes that are significantly upregulated in the EPO-responder group, when compared to control and non-responder groups. Differential expression was assessed using a logistic regression testing approach, as implemented in Seurat.

Figure 6: EPO-responders are multipotent progenitors, not HSCs. Same protocol as in Figure 5**. a,** Expression of published gene-signatures of HSCs (dormant HSC[57],

molecular overlap (molO) HSC signature[58]) and MPPs (MPP1[57]-2[31]) across the entire dataset (see Supplementary Methods) **b**, Expression of the signatures from 6a, across control, non-responder, and EPO-responder groups as defined in Figure 5c. Statistical comparisons made using a Kruskal Wallis Test with a Dunns multiple comparisons post-hoc test **c**, Expression of the molO HSC signature on the published reference map[51]. **d**, Nearest-neighbor mapping of control, EPO-responder and non-responder cells onto the published reference map[51].

Figure 7: The effect of EPO on HSPC clonality after transplantation is transient. Same protocol as in Figure 2, but barcodes in the E, M, and B lineage in spleen of individual mice sacrificed at month 4 post-transplantation were analyzed. **a**, Triangle plots showing the relative abundance of barcodes (circles) in the erythroid (E), myeloid (M), and B-cell (B) lineage with respect to the summed output over the three lineages (size of the circles) for the different experimental groups as indicated. **b**, The percentage of each lineage produced by the barcodes categorized by bias using a 10% threshold. **c**, The fraction of donor cells among the indicated cell types in spleen. **d**, Barcode number retrieved in the indicated lineage at month 4 after transplantation in control (black dot), EPO 160 ng/ml (red square), and EPO 1,000 ng/ml (red triangle) group. **e**, Percentage of HSPCs classified using a threshold of 10% in experimental groups as indicated. Shown are data from several mice. (c, n=5 for control and n=4 for each EPO group, (a-b, d-e) n=6 for control and n=4 for each EPO group (collected over two experiments)). For all bar graphs mean and S.D. between mice are depicted. Statistical significance tested using Student-T-test p=0,05 for (c-e).

Figures

Figure 1

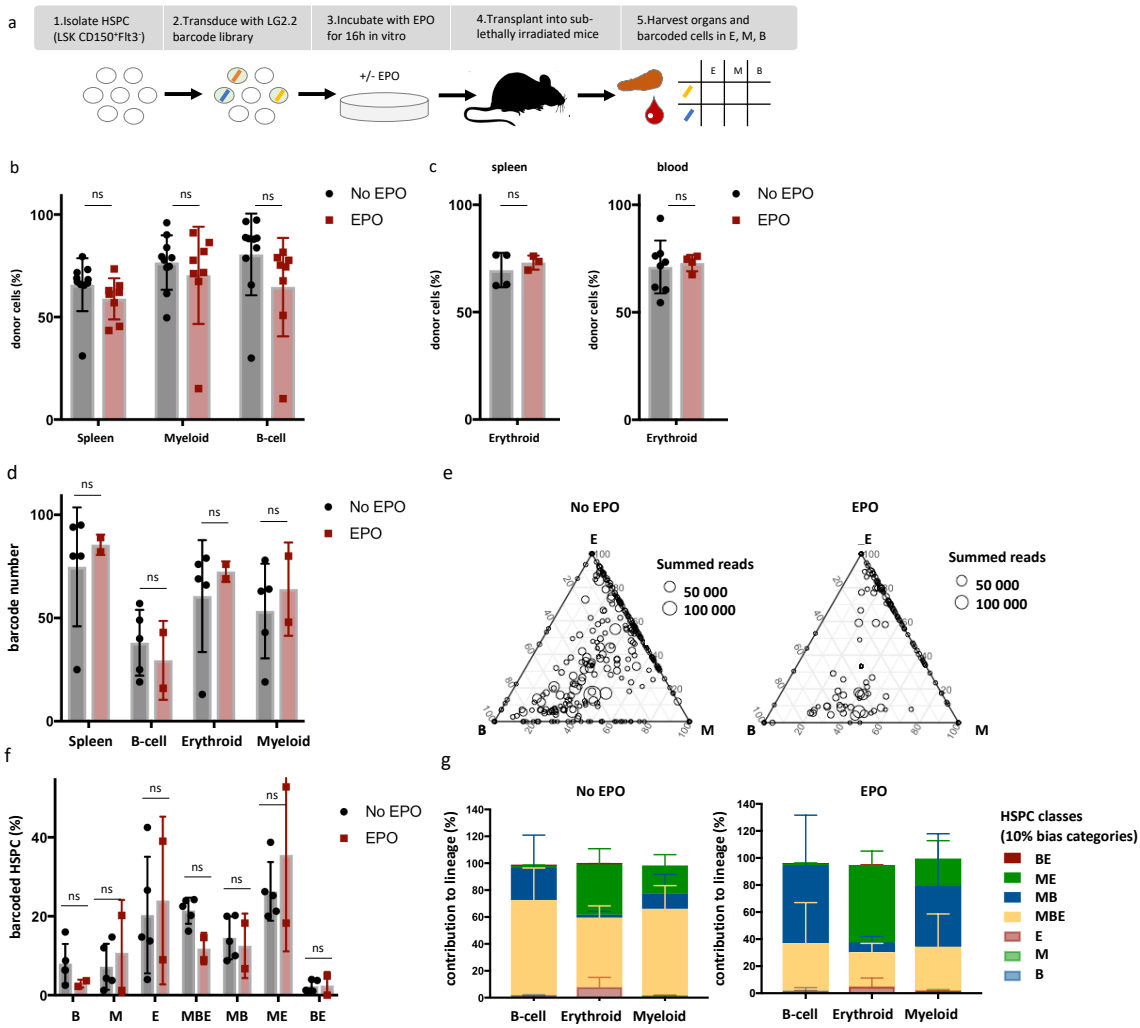
a
1.Isolate HSPC (LSK CD150+Flt3-)
2.Transduce with LG2.2 barcode library
3.Incubate with EPO for 16h in vitro
4.Transplant into sub-lethally irradiated mice
5.Harvest organs and barcoded cells in E, M, B
+/- EPO
E
M
B
b
donor cells (%)
ns
No EPO
EPO
Spleen
Myeloid
B-cell
c
spleen
blood
Erythroid
d
barcode number
B-cell
Erythroid
Myeloid
e
No EPO
EPO
Summed reads
50 000
100 000
f
barcoded HSPC (%)
B
M
E
MBE
MB
ME
BE
g
contribution to lineage (%)
HSPC classes
(10% bias categories)
BE
ME
MB
MBE
E
M
B

Figure 2

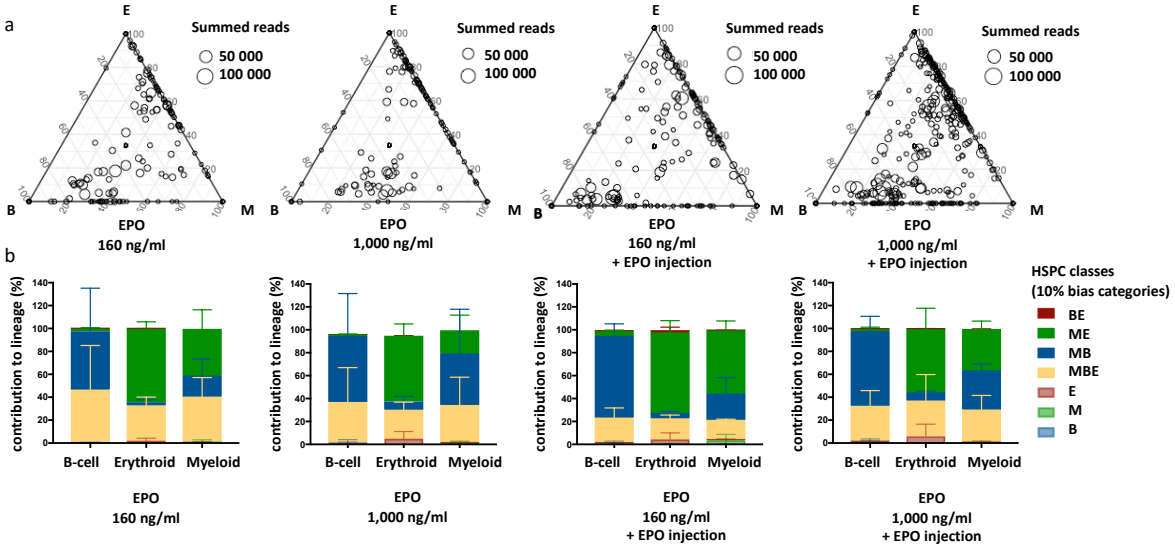
a
E
B
M
Summed reads
50 000
100 000
EPO
160 ng/ml
EPO
1,000 ng/ml
EPO
160 ng/ml
+ EPO injection
EPO
1,000 ng/ml
+ EPO injection
b
contribution to lineage (%)
B-cell
Erythroid
Myeloid
HSPC classes
(10% bias categories)
BE
ME
MB
MBE
E
M
B

Figure 3

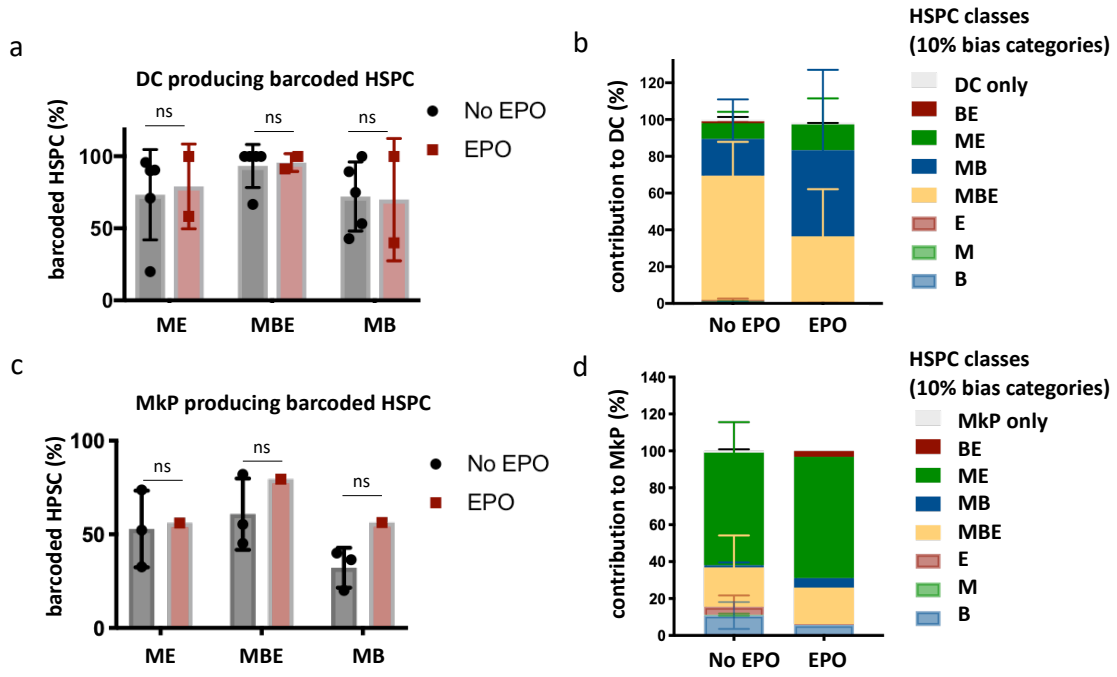
a
DC producing barcoded HSPC
barcoded HSPC (%)
ns
ns
ns
No EPO
EPO
ME
MBE
MB
b
contribution to DC (%)
HSPC classes
(10% bias categories)
DC only
BE
ME
MB
MBE
E
M
B
No EPO
EPO
c
MkP producing barcoded HSPC
barcoded HPSC (%)
ns
ns
ns
No EPO
EPO
ME
MBE
MB
d
contribution to MkP (%)
HSPC classes
(10% bias categories)
MkP only
BE
ME
MB
MBE
E
M
B
No EPO
EPO

Figure 4

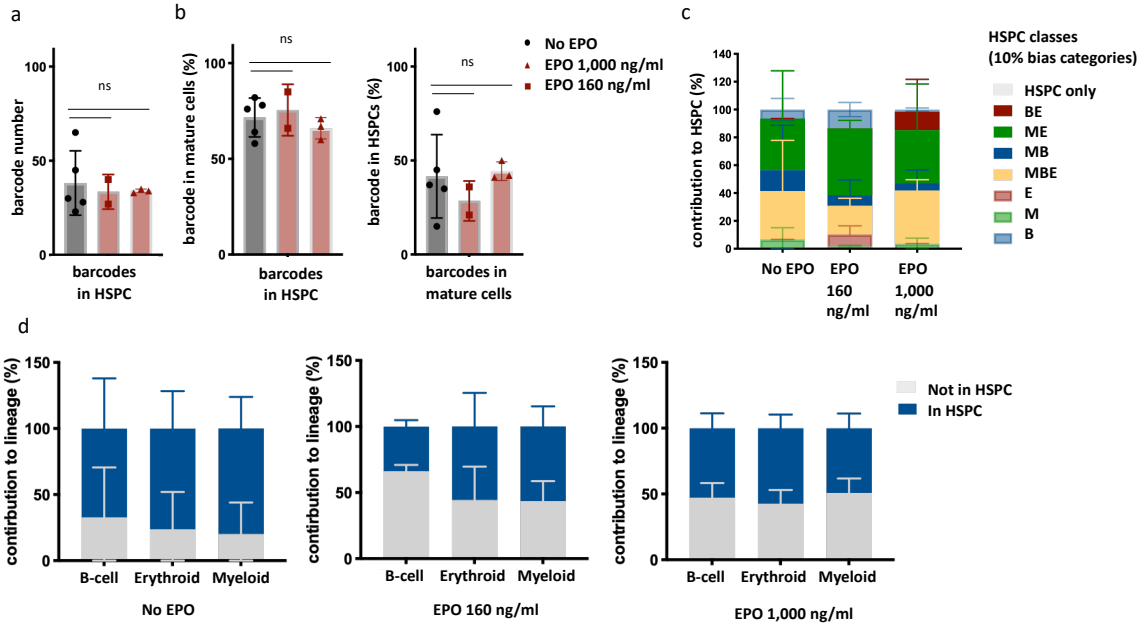
a
b
c
d
barcode number
barcodes in HSPC
barcode in mature cells (%)
barcodes in HSPC
barcode in HSPCs (%)
barcodes in mature cells
ns
No EPO
EPO 1,000 ng/ml
EPO 160 ng/ml
contribution to HSPC (%)
No EPO
EPO 160 ng/ml
EPO 1,000 ng/ml
HSPC classes (10% bias categories)
HSPC only
BE
ME
MB
MBE
E
M
B
contribution to lineage (%)
B-cell
Erythroid
Myeloid
No EPO
EPO 160 ng/ml
EPO 1,000 ng/ml
Not in HSPC
In HSPC

Figure 5

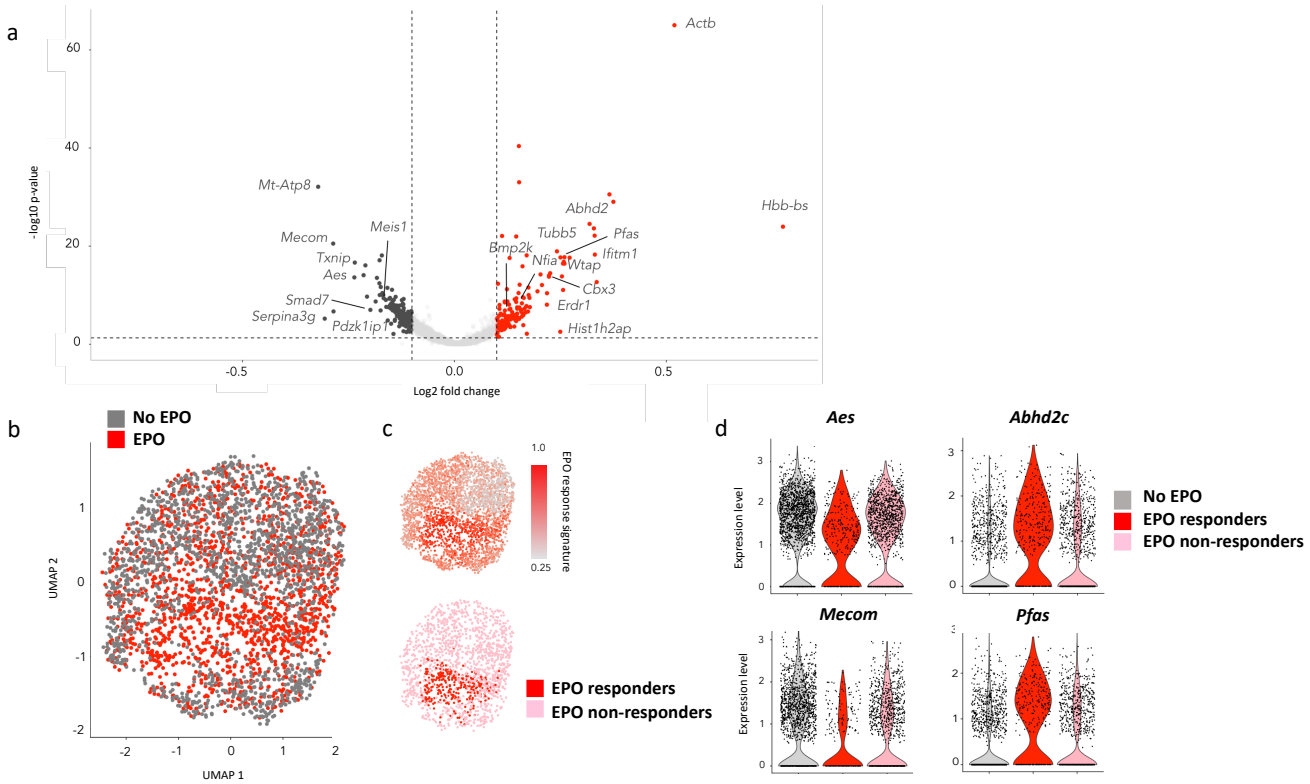
a
Actb
Mt-Atp8
Meis1
Mecom
Txnip
Aes
Smad7
Serpina3g
Pdzk1ip1
Abhd2
Tubb5
Pfas
Bmp2k
Nfia
Ifitm1
Wtap
Cbx3
Erdr1
Hist1h2ap
Hbb-bs
-log10 p-value
Log2 fold change
b
No EPO
EPO
UMAP 1
UMAP 2
c
EPO response signature
EPO responders
EPO non-responders
d
Aes
Abhd2c
Mecom
Pfas
Expression level
No EPO
EPO responders
EPO non-responders

Figure 6

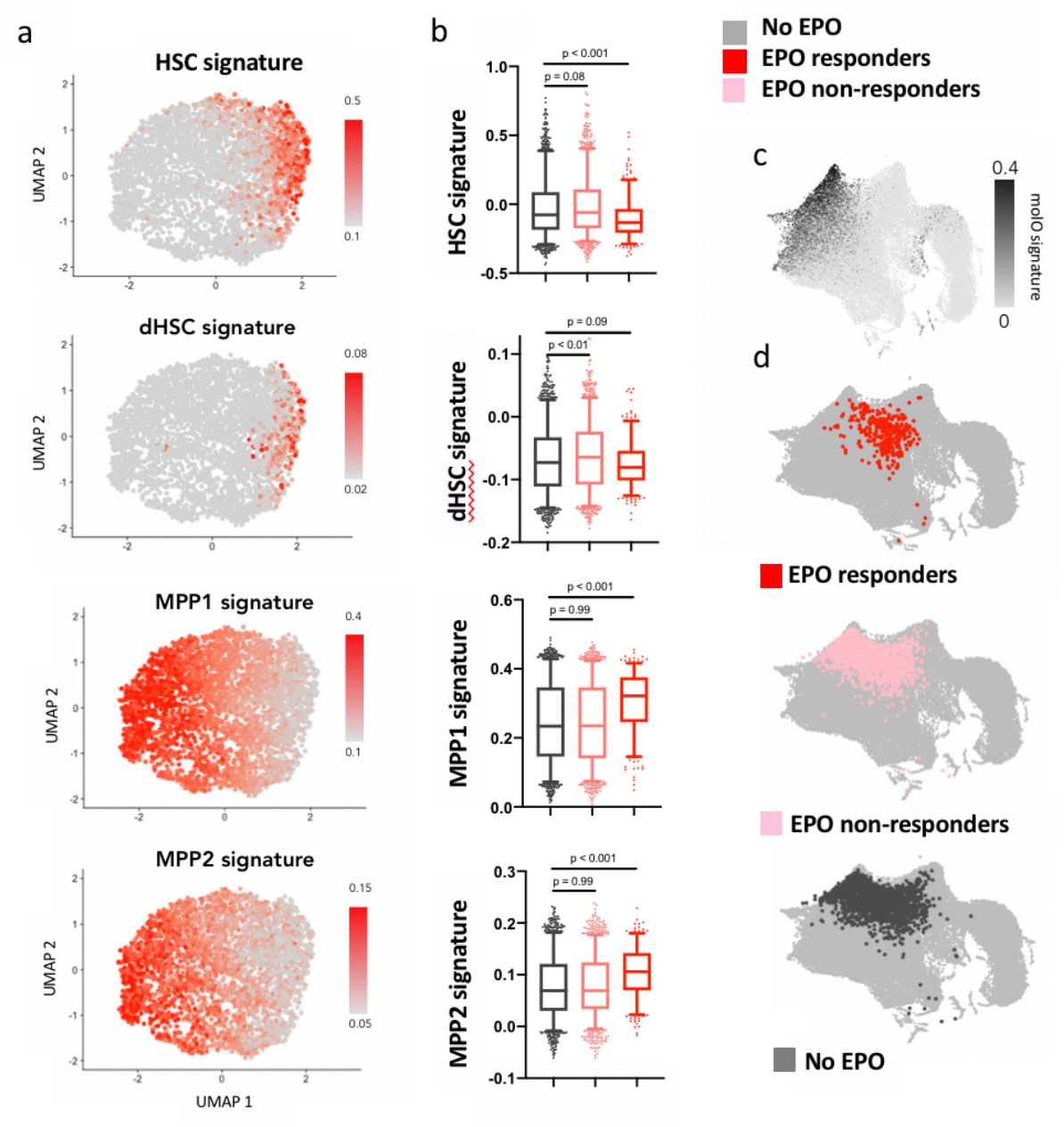
a
HSC signature
dHSC signature
MPP1 signature
MPP2 signature
UMAP 2
UMAP 1
b
HSC signature
dHSC signature
MPP1 signature
MPP2 signature
p < 0.001
p = 0.08
p = 0.09
p < 0.01
p = 0.99
No EPO
EPO responders
EPO non-responders
c
molO signature
d
EPO responders
EPO non-responders
No EPO

Figure 7

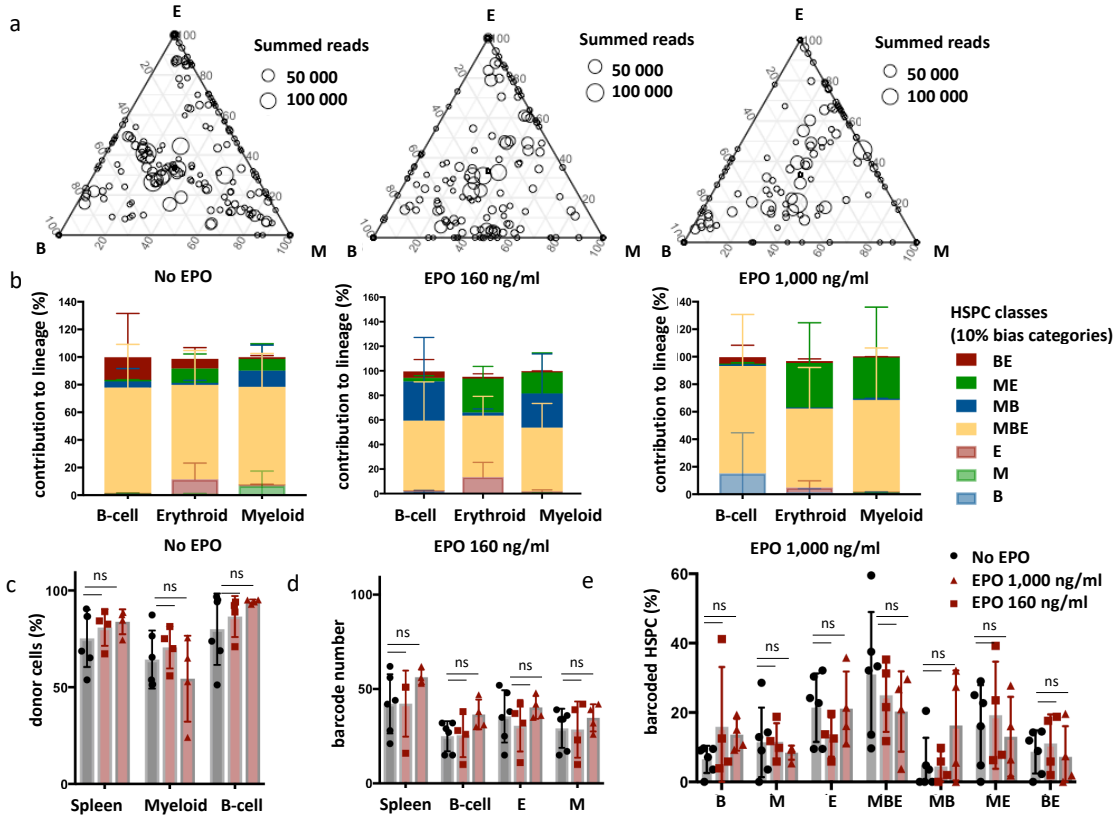
a
E
B
M
Summed reads
50 000
100 000
No EPO
EPO 160 ng/ml
EPO 1,000 ng/ml
b
contribution to lineage (%)
B-cell
Erythroid
Myeloid
HSPC classes
(10% bias categories)
BE
ME
MB
MBE
E
M
B
c
donor cells (%)
ns
Spleen
Myeloid
B-cell
d
barcode number
Spleen
B-cell
E
M
e
barcoded HSPC (%)
No EPO
EPO 1,000 ng/ml
EPO 160 ng/ml
B
M
E
MBE
MB
ME
BE